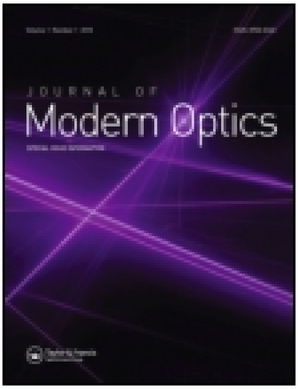

Journal of Modern Optics
Publication details, including instructions for authors and subscription information:
http://www.tandfonline.com/loi/tmop20

Phase Shifting Scatter Plate Interferometer Using a Polarization Technique

Der-Chin Su [a] & Lih-Horng Shyu [a]
[a] Institute of Electro-Optical Engineering , National Chiao-Tung University , 1001, Ta-Hsueh Road, Hsin-chu, Taiwan, Republic of China
Published online: 01 Mar 2007.

To cite this article: Der-Chin Su & Lih-Horng Shyu (1991) Phase Shifting Scatter Plate Interferometer Using a Polarization Technique, Journal of Modern Optics, 38:5, 951-959, DOI: 10.1080/09500349114550931

To link to this article: http://dx.doi.org/10.1080/09500349114550931

JOURNAL OF MODERN OPTICS, 1991, VOL. 38, NO. 5, 951–959

Phase shifting scatter plate interferometer using a polarization technique

DER-CHIN SU and LIH-HORNG SHYU
Institute of Electro-Optical Engineering,
National Chiao-Tung University,
1001 Ta-Hsueh Road, Hsin-chu, Taiwan, Republic of China

(*Received 19 June 1990; revision received 22 August 1990*)

Abstract. The structure of a conventional scatter plate interferometer is modified by a polarization technique, and a new type of phase shifting scatter plate interferometer is presented. It has both the merits of a conventional scatter plate interferometer and the phase shifting interferometric technique. The working of this interferometer is demonstrated.

1. Introduction

In digital phase shifting interferometry [1–4], the phase difference between the two interfering beams is varied in some known manner, and the measurements are made of the intensity distribution across the pupil corresponding to three or more different phase shifts. If the values of these external phase shifts are known, then it is possible to calculate the initial phase difference between the interfering beams.

In a two-path interferometer, such as a Twyman–Green interferometer, it is very easy to use a piezoelectic transducer (PZT) as a phase shifter. But in a scatter plate interferometer [5–7], it is very difficult to use a PZT as a phase shifter due to its common path configuration. In order to solve this problem, Huang *et al.* [4] located a very small quarter wave plate just before the centre of the test mirror and made the reference beam pass through the quarter wave plate twice; then the phase difference between the test beam and the reference beam may be varied according to the polarization angle of the incident beam. However, there are some disadvantages in Huang's apparatus, such as:

(i) It is difficult to get that quarter wave plate with a special specification, e.g., 0·05 mm thickness and $5 \times 5\,\mathrm{mm}^2$ area.
(ii) It is also difficult to hold it without blocking off part of the test beam.
(iii) The quarter wave plate can not be brought to a full effect, because the beam passing through it is not a parallel beam.

In this paper, in contrast to Huang's technique, a polarizer with a small hole is located before the test mirror. And a half wave plate and a quarter wave plate are added before the projection lens. This modification has several advantages. First, the polarizer can extract the linearly polarized light lying in the plane of transmission from any incident beam independent of the beam vergence. Second, a large polarizer is easy to hold without blocking off part of the test beam. Furthermore, if the azimuth angle of every polarization element is arranged properly, then the phase shifting interferometric technique can be applied to the scatter plate interferometer.

2. Principle

The schematic diagram of a new type of phase shifting scatter plate interferometer is shown in figure 1. If the polarization components H, Q, PL, and AN are removed, then it is a conventional scatter plate interferometer [6, 7]. The linearly polarized light passes through a half wave plate H and a quarter wave plate Q, then goes into the scatter plate interferometer. The polarizer PL is adjusted such that the small hole be just before the centre of the test mirror M. Therefore, the test beam passes through PL twice. The analyser AN is put before the observation plane OP to extract the necessary polarizing components to interfere. Hence, the phase map of the test mirror can be derived from the interferograms.

For convenience, the $+z$ axis is chosen along the propagation direction and the y-axis along the vertical direction. Let the incident light be linearly polarized along the horizontal direction, then its Jones vector [8] can be written as

$$\mathbf{E}_{\text{in}} = \begin{pmatrix} 1 \\ 0 \end{pmatrix}. \tag{1}$$

If θ_h is the angle between the x axis and the fast axis of the half wave plate H, and θ_q is the angle between the x axis and the fast axis of the quarter wave plate Q, then the Jones matrices [8] of H and Q can be written as

$$H(\theta_h) = -\mathrm{i}\begin{pmatrix} \cos 2\theta_h & \sin 2\theta_h \\ \sin 2\theta_h & -\cos 2\theta_h \end{pmatrix}, \tag{2}$$

and

$$\mathbf{Q}(\theta_q) = \frac{\sqrt{2}}{2}\begin{pmatrix} 1-\mathrm{i}\cos 2\theta_q & -\mathrm{i}\sin 2\theta_q \\ -\mathrm{i}\sin 2\theta_q & 1+\mathrm{i}\cos 2\theta_q \end{pmatrix}, \tag{3}$$

respectively. Let the angle between the x axis and the transmission axis of the polarizer PL be θ_p, then since the test beam passes PL twice, hence the Jones matrix of PL can be written as

$$\begin{aligned} \mathbf{PL}(\theta_p) &= \mathbf{R}(-\theta_p)\begin{pmatrix} 1 & 0 \\ 0 & 0 \end{pmatrix}\begin{pmatrix} 1 & 0 \\ 0 & 0 \end{pmatrix}\mathbf{R}(\theta_p) \\ &= \begin{pmatrix} \cos^2\theta_p & \sin\theta_p\cos\theta_p \\ \sin\theta_p\cos\theta_p & \sin^2\theta_p \end{pmatrix}, \end{aligned} \tag{4}$$

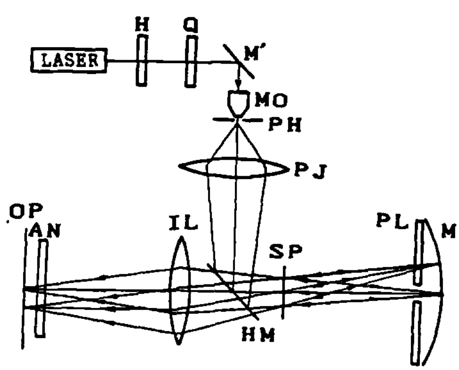

Figure 1. Schematic diagram of a phase shifting scatter plate interferometer. H: half wave plate. Q: quarter wave plate. M: mirror. MO: microscopic objective. PH: pinhole. PJ: projection lens. HM: half mirror. SP: scatter plate. PL: polarizer. M: mirror to be tested. IL: imaging lens. AN: analyser. OP: observation plane.

where

$$\mathbf{R}(\theta_p)=\begin{pmatrix}\cos\theta_p & \sin\theta_p\\ -\sin\theta_p & \cos\theta_p\end{pmatrix}$$

is the rotation matrix. Similarly, since the transmission axis of the analyser AN is along the horizontal axis, hence the Jones matrix of AN is

$$\mathbf{AN}(0)=\begin{pmatrix}1 & 0\\ 0 & 0\end{pmatrix}. \tag{5}$$

Therefore, the Jones vector of the test beam in the observation plane is

$$\mathbf{E}_t=a\exp[i\alpha(x,y)]\,\mathbf{AN}(0)\mathbf{PL}(\theta_p)\mathbf{Q}(\theta_q)\mathbf{H}(\theta_h)\mathbf{E}_{in}, \tag{6}$$

where a is the amplitude of the test beam relative to the reference beam and $\alpha(x,y)$ is the phase difference of the test beam relative to the reference beam. For convenience, the amplitude of the reference beam is normalized to 1.

By inserting the matrices written in equations (2)–(5) into equation (6), $\mathbf{E}_t$ can be written as

$$\mathbf{E}_t=\begin{pmatrix}A\exp[i(\alpha-\Psi_t)]\\ 0\end{pmatrix}, \tag{7}$$

where

$$A=af_1(\theta_h,\theta_q,\theta_p), \tag{8}$$

$$f_1(\theta_h,\theta_q,\theta_p)=\frac{\sqrt{2}}{2}\cos\theta_p[\cos^2(\theta_p-2\theta_h)+\cos^2(\theta_p-2\theta_q+2\theta_h)]^{1/2}, \tag{9}$$

and

$$\Psi_t=\tan^{-1}\left[\frac{\cos(\theta_p-2\theta_q+2\theta_h)}{\cos(\theta_p-2\theta_h)}\right]+\frac{\pi}{2}. \tag{10}$$

Similarly, the Jones vector of the reference beam in the observation plane is given by

$$\mathbf{E}_r=\mathbf{AN}(0)\mathbf{Q}(\theta_q)\mathbf{H}(\theta_h)\mathbf{E}_{in}=\begin{bmatrix}B\exp(-i\Psi_r)\\ 0\end{bmatrix}, \tag{11}$$

where

$$B=f_2(\theta_h,\theta_q), \tag{12}$$

$$f_2(\theta_h,\theta_q)=\frac{\sqrt{2}}{2}[\cos^2(2\theta_q-2\theta_h)+\cos^2(2\theta_h)]^{1/2}, \tag{13}$$

and

$$\Psi_r=\tan^{-1}\left[\frac{\cos(2\theta_q-2\theta_h)}{\cos(2\theta_h)}\right]+\frac{\pi}{2}. \tag{14}$$

Therefore, the intensity distribution of the interferogram is obtained as following

$$\begin{aligned} I &= |\mathbf{E}_t + \mathbf{E}_r|^2 \\ &= A^2 + B^2 + 2AB\cos(\alpha + \Delta\Psi), \end{aligned} \tag{15}$$

where

$$\Delta\Psi = \Psi_r - \Psi_t. \tag{16}$$

From equations (10), (14), and (16) it can be seen that $\Delta\Psi$ represents the external phase shift corresponding to the variations of the azimuth angles of the polarization components. The method of selecting the appropriate angles to obtain the initial phase α will be described in the following.

2.1. *Selection of the azimuth angles*

From equation (9), it is clear that the amplitude of the test beam af_1 depends on θ_p. In order to have a non-zero f_1, θ_p should satisfy the following condition,

$$\theta_p \neq N\pi + \frac{\pi}{2}, \tag{17}$$

where N is an integer. Furthermore, by comparing equation (9) and equation (13), it is noticed that, under the condition

$$\theta_p = 2\theta_q = \text{constant}, \tag{18}$$

the amplitudes of the test beam and the reference beam have the same functional form of θ_h. This makes the evaluation of the initial phases easier. However, by comparing equation (10) and equation (14), it is seen that if θ_p equals $N\pi$, there will be no external phase shift. Hence, θ_p should be chosen such that it satisfies both equation (17) and the following equation simultaneously,

$$\theta_p \neq N\pi. \tag{19}$$

Under the conditions written in equations (17)–(19), equation (15) and equation (16) can be rewritten as

$$I = I_0(\theta_h)[1 + \gamma\cos(\alpha + \Delta\Psi)], \tag{20}$$

and

$$\Delta\Psi = \tan^{-1}\left[\frac{\cos(\theta_p - 2\theta_h)}{\cos(2\theta_h)}\right] - \tan^{-1}\left[\frac{\cos(2\theta_h)}{\cos(\theta_p - 2\theta_h)}\right], \tag{21}$$

where

$$I_0(\theta_h) = \left[\frac{\cos^2(2\theta_h) + \cos^2(\theta_p - 2\theta_h)}{2}\right] \times (1 + a^2\cos^2\theta_p), \tag{22}$$

and

$$\gamma = \frac{2a\cos\theta_p}{1 + a^2\cos^2\theta_p}. \tag{23}$$

From equation (20), it is seen that γ represents the contrast of the interference fringes. Equation (21) shows that if θ_p is set to be a constant, then $\Delta\Psi$ is a function of

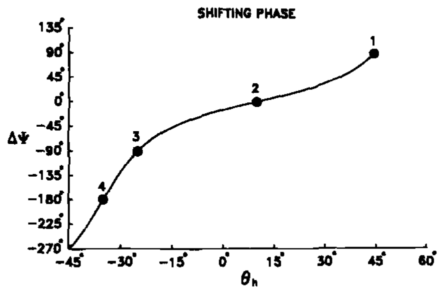

Figure 2. Variations of the external phase shift $\Delta\Psi$ as a function of θ_h, as $\theta_p = 40°$.

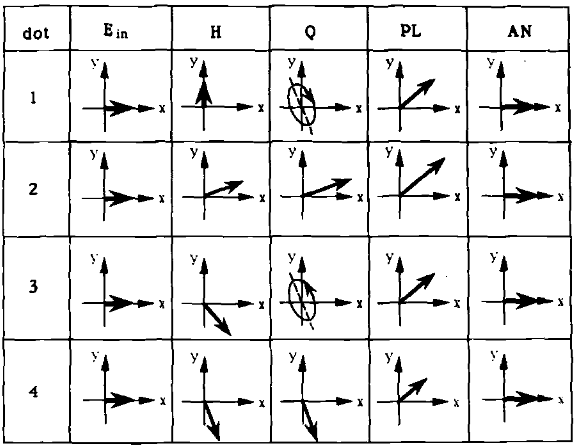

Figure 3. The polarization states of the light through every polarization element under the conditions corresponding to dot 1 to dot 4 in figure 2.

θ_h with a period of 90°: $-45° \leqslant \theta_h \leqslant 45°$ is chosen for convenience. Furthermore, equation (21) also shows that when θ_h equals 45°, $\frac{\theta_p}{4}$, $\frac{\theta_p}{2} - 45°$ and $\frac{\theta_p}{4} - 45°$, $\Delta\Psi$ equals 90°, 0°, −90° and −180°, respectively. For easier calculation and operation, $\theta_p = 40°$ is chosen. Then the corresponding θ_h are 45°, 10°, −25° and −35°, respectively. The relation between $\Delta\Psi$ and θ_h calculated for this θ_p is shown in figure 2. And the four points marked from 1 to 4 correspond to the angle θ_h at 45°, 10°, −25° and −35°. For clarity, the polarization states of the light through every polarization element under the conditions corresponding dot 1 to dot 4 are shown in figure 3.

2.2. *Evaluation of the initial phases*

As described in the previous paragraph, the conditions corresponding to dot 1 to dot 4 in figure 2 are chosen such that the $\Delta\Psi$ at these points equals 90°, 0°, −90° and −180°, respectively. Then the corresponding interferograms can be calculated by using equation (20). They are written as following:

$$I_1 = \frac{\sin^2\theta_p}{2}(1 + a^2\cos^2\theta_p)(1 - \gamma\sin\alpha), \tag{24}$$

$$I_2 = \cos^2\left(\frac{\theta_p}{2}\right)(1 + a^2\cos^2\theta_p)(1 + \gamma\cos\alpha), \tag{25}$$

$$I_3 = \frac{\sin^2\theta_p}{2}(1 + a^2\cos^2\theta_p)(1 + \gamma\sin\alpha), \tag{26}$$

and

$$I_4 = \sin^2\left(\frac{\theta_p}{2}\right)(1 + a^2\cos^2\theta_p)(1 - \gamma\cos\alpha). \tag{27}$$

Finally, combining equations (24)–(27), the initial phase is given by

$$\alpha = \tan^{-1}\left\{\frac{2(I_3 - I_1)/\sin^2\theta_p}{\left[I_2/\cos^2\left(\frac{\theta_p}{2}\right)\right] - \left[I_4/\sin^2\left(\frac{\theta_p}{2}\right)\right]}\right\}. \tag{28}$$

2.3. *An additional phase error*

Because of the introduction of the polarizer located before the test surface, it introduces an additional optical path and there will be an additional phase error in α. The interferograms obtained with this method indicate the gross wavefront errors. The additional phase error should be eliminated. If the thickness and the refraction index of the polarizer are t and n, then the additional phase error can be written as

$$\Delta \doteqdot \frac{2\pi}{\lambda}\left[2t(n-1) + t\left(1 - \frac{1}{n}\right)\left(\frac{p}{r}\right)^2 + t\left(\frac{1}{n} - \frac{1}{4n^3} - \frac{3}{4}\right)\left(\frac{p}{r}\right)^4 + \dots\right],$$

$$= \Delta_1 + \Delta_2 + \Delta_3 + \dots, \tag{29}$$

where p is the distance between a point and the centre on the test surface, and r is the paraxial radius of curvature of the test surface. The first term Δ_1 in equation (29) is a constant, it adds a constant to the phase of each point on the test surface. It changes the level of the phase of reference plane, but the shape of the overall phase distribution is unchanged. Hence it can be neglected in evaluating the initial phase. The second term Δ_2 has the same effect on the result as the defocus of the scatter plate [9]. It can be eliminated experimentally by defocusing the scatter plate by an amount of $t[(1-(1/n)]$ away from the test mirror. Therefore, the factor that affects the accuracy of the phase map α is the third term Δ_3. However, this error can be calculated for each position p from known polarizer parameters t and n and the paraxial radius r of curvature of the test mirror. Thus, the original phase map of the test mirror can be obtained.

3. Experiments and results

To show the feasibility of this phase shifting scatter plate interferometer, a spherical mirror of $f/5$ and focal length 250 mm is tested. The diameter of the small hole on the polarizer is 3 mm. The thickness of the polarizer is 3·2 mm, and the refraction index 1·515. And the experimental conditions are $\theta_p = 2\theta_q = 40°$, $\theta_h = 45°$, 10°, −25° and −35°, respectively. To set the azimuth angle accurately, high precision holders manufactured by Japan Sigma Koki Ltd are used to mount the polarization elements. (Σ-58M-30 and Σ-58M-50 are used to mount the waveplate and the polarizer, respectively). And the scatter plate is defocused nearly 1·1 mm away from the test mirror to eliminate the influence of Δ_2. Then, four interferograms, being under the condition that the scatter plate is slightly off-axis, are shown in figure 4. They correspond to $\Delta\Psi = (a)$ 90°, (b) 0°, (c) −90° and (d) 180°,

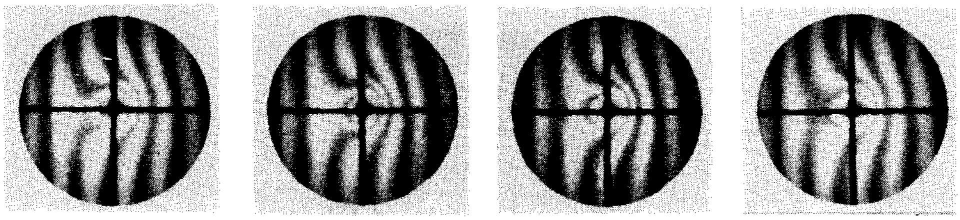

(*a*) (*b*) (*c*) (*d*)

Figure 4. Interferograms of an $f/5$ spherical mirror with 250 mm focal length when the scatter plate is slightly off-axis and $\Delta\Psi$ equals (*a*) 90°, (*b*) 0°, (*c*) −90° and (*d*) −180°, respectively. (The black cross is the reticle on the image plane).

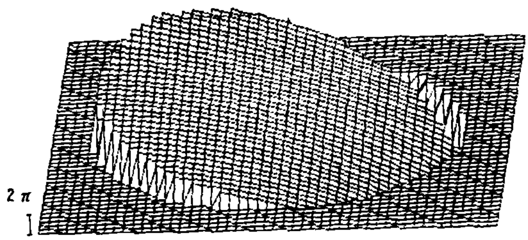

Figure 5. The phase map of the test mirror.

respectively. The phase shifting effects are clear from these interferograms. These interferograms are taken by a CCD camera, recorded in a frame memory, then sent to a computer. Using equation (28), the initial phase α is obtained. The phase error Δ_3 at each point is calculated and subtracted from α to obtain the original phase. The final result is plotted in figure 5. In this plotting, the characteristics [10] of continuous phase distribution is applied and the 3-D software 'ENERGRAPHIC' is used.

4. Discussion

Because of the introduction of a polarization element located before the test surface, there is thus an addition phase error in Huang's technique and ours. Also, the quality requirements of polarization elements, such as the flatness of surfaces and the parallelism between two surfaces, are very restrictive. In Huang's technique, the additional phase error comes from only the first term in equation (29), and can be eliminated more easily. However, the main disadvantage of Huang's technique is that it is difficult both to get and to hold a quarter wave plate because of its specification. In addition, because the wave plate is located near the focus of the converging light, the light reflected from the front surface of it will reduce the fringe contrast. And the fringes near the central part of the test surface can hardly be observed.

On the other hand, the measurable range of our technique is limited by the dimension of the high-quality polarizer. Also, there are some curvatures among the

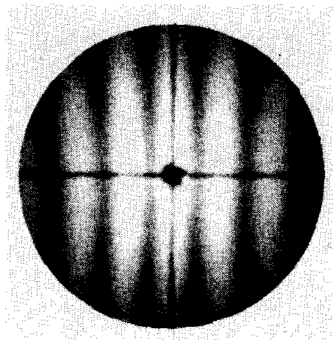

Figure 6. The interferogram of the same mirror tested by a conventional scatter plate interferometer.

fringes near the central part of the interferograms. This is induced by the small hole on the polarizer. However, the dimension of this part is small and the *f*-number is large. Hence, this part can be easily tested by any conventional interferometer. The interferograms here are analysed under the assumption that there is no shape error near the central part of the test surface.

In order to identify the result shown in figure 5, the same mirror is tested by a conventional scatter plate interferometer and an interferogram is obtained as shown in figure 6. It is obvious that this interferogram shows phase characteristics similar to that in figure 5.

5. Conclusion

To overcome the difficulty of using a commonly used phase shifter PZT, a new type of phase shifting scatter plate interferometer using a polarization technique is presented. A spherical mirror of $f/5$ and focal length 250 mm has been tested to demonstrate the operation of the interferometer. It has both the merits of a conventional scatter plate interferometer and the phase shifting interferometric technique, such as high stability against the air turbulence, high measurement accuracy, rapid measurement and good results even with low contrast fringes, . . . etc. Hence it is suitable for testing a concave mirror. Furthermore, other similar common path interferometers, such as a zone plate interferometer, can be modified with the same way.

Acknowledgments

We thank the National Science Council, R.O.C. for their support of this work, and thank Dr Huang [4] for his useful discussions and suggestions.

References

[1] Bruning, J. H., Herriott, D. R., Gallagher, J. E., Rosenfeld, D. P., White, A. D., and Brangaccio, D. J., 1974, *Appl. Optics*, **13**, 2693.
[2] Hariharan, P., Oreb, B. F., and Leistner, A. J., 1984, *Opt. Engng*, **23**, 294.
[3] Hariharan, P., 1987, *Proc. SPIE*, **813**, 11.

[4] HUANG, J., HONDA, T., OHYAMA, N., and TSUJIUCHI, J., 1988, *Opt. Commun.*, **68**, 235.
[5] BURCH, J. M., 1962, *J. opt. Soc. Am.*, **52**, 600.
[6] RUBIN, L., 1980, *Appl. Optics*, **19**, 1634.
[7] SU, D. C., OHYAMA, N., HONDA, T., and TSUJIUCHI, J., 1986, *Optics Commun.*, **58**, 139.
[8] YARIV, A., and YEH, P., 1984, *Optical Waves in Crystals* (New York: Wiley), ch. 5.
[9] SU, D. C., HONDA, T., and TSUJIUCHI, J., 1984, *Optics Commun.*, **50**, 137.
[10] TAKEDA, M., INA, H., and KOBAYASHI, S., 1982, *J. opt. Soc. Am.*, **72**, 156.